John E. Estes
University of California
Santa Barbara, CA 93106
Michael R. Mel
Escatech
Playa del Key, CA 90291
John O. Hooper
Naval Weapons Center
China Lake, CA 93555

Measuring Soil Moisture with an Airborne Imaging Passive Microwave Radiometer

Statistically highly significant linear correlation exists between image tone density and moisture content in the top 5 cm of the soil.

Introduction

This paper presents the results of a limited experiment to determine if a statistically significant relationship between image gray tone level and soil moisture exists on imagery from a 35 GHz scanning passive microwave radiometer. Experimental results are encouraging. However, additional tests need to be conducted using a larger sample with more diverse terrain types and conditions in order to assess the impact of differing amounts of vegetation cover on soil moisture/signature correlation. In July 1973 the Geography Remote Sensing Unit, University of California, Santa Barbara, received a contract from the Naval Weapons Center (N.W.C.), China Lake, California, to evaluate the potential of an Aerojet Electrosystems-built microwave radiometer which had been modified by the Microwave Laboratory at N.W.C. China Lake. The basic purpose of the experiments conducted under this program was to test the system's capabilities as a navigational aid.[1] In the course of fulfilling this contract, the Geography Remote Sensing Unit was encouraged by our Naval Weapons Center monitors to evaluate some of the broader environmental applications of the system as well. As such, in February 1974 a soil moisture sampling experiment was performed; the samples were taken from bare soil fields on a transect along Lost Hills Road on the West Side of the San Joaquin Valley, California (Figure 1). The experiment arose from the continuing problem faced by hydrologists, meteorologists, geologists, and others interested in measuring soil moisture in obtaining reliable data over large or inaccessible areas. Spatial variations in soil moisture may be particularly crucial in an agricultural situation where an adequate water balance is critical to plant physiology. Short of exhaustive field sampling, no dependable method for gathering regional soil moisture data presently exists.

Abstract: *Short of exhaustive field sampling, no dependable method for gathering regional soil moisture data presently exists. Passive microwave remote sensing technology has the ability to provide areally extensive information on near-surface soil moisture condition. Experiments conducted with an imaging passive microwave radiometer on the West Side, San Joaquin Valley, California, indicate that a statistically highly significant linear correlation exists between image tone density and moisture content in the top 5 cm of the soil. Further, this relationship may be seen to intensify somewhat when soils are subdivided by type and show a slightly stronger correlation for the less coarse of the two soil types present.*

Photogrammetric Egineering and Remote Sensing,
Vol. 43, No. 10, October 1977, pp. 1273-1281.

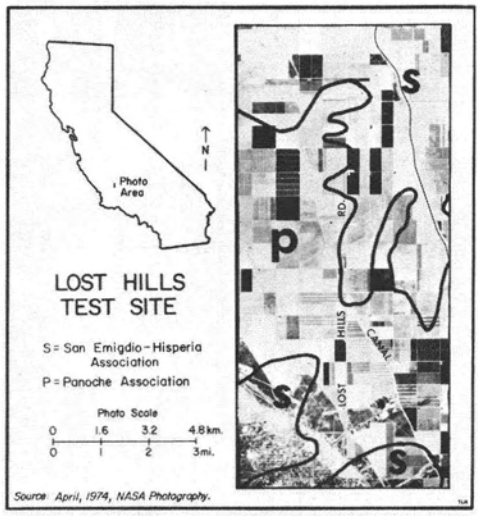

FIG. 1. Aerial photograph with an overlay of soil boundaries as mapped by the Soil Conservation Service. P corresponds to the Panoche soil association, while S indicates the coarser San Emigdio soil type. Other features labeled may be correlated to those same features as they appear on the MICRAD images in Figures 5 and 6.

Experiments with remote sensing techniques have tested the potential of various systems for monitoring soil moisture conditions from airborne platforms. Among techniques tested, several papers have appeared detailing the relationship between soil moisture and energy balance at microwave wavelengths.[2] Passive microwave sensors image energy emitted, reflected, and transmitted from a scene. Owing to the difference in the dielectric constant of water, which may be as much as 80 at microwave frequencies, and dry soil which is typically less than 5, the amount of moisture contained in a given soil can greatly affect its dielectric properties. Resulting emissivities for a bare smooth field may range from 0.5 for a wet soil to greater than 0.9 for a dry soil.[3] It is these variations which are basically responsible for the differences in tone between wet and dry fields which appear on passive microwave images. Whereas experiments indicate that passive microwave remote sensors show promise in this area, no thorough analysis of the ability of such a relatively high resolution scanning system to produce areally extensive soil moisture has yet been accomplished. One reason for this situation is that many airborne passive microwave radiometer systems currently in use "look" at a single fixed swath of terrain directly below the aircraft. Microwave signal intensities are integrated over the swath width sensed by the fixed antenna. The output consists of a graph that plots brightness temperature along the vertical axis with distance along the horizontal axis. The potential for the generation of really extensive data is therefore lost. Even where scanning antennas have been employed, resolutions have been relatively coarse. Information gathered by many scanning systems is displayed as a series of rectangles which have been coded with a symbol or color representing the relative intensity of microwave energy emanating from the scene. Recently, however, data from the Naval Weapons Center high-resolution imaging system has become available for study. The resolution element of this system is much smaller than earlier systems, which greatly increases the detail and information content of the resultant microwave radiometric (MICRAD) images. The essential advantage of the imaging passive MICRAD system is that it produces an image which displays the relative microwave intensities of terrain features in a geographic context, rather than "averaging" the view for a given scene and presenting its output in graph or coded form. The product of this system is an actual image which bears a marked resemblance to imagery produced by systems operating in the thermal infrared portion of the electromagnetic spectrum. This image provides the interpreter with a more familiar frame of reference within which to analyze the distribution of intensities presented.

MICROWAVE ENERGY AND SENSOR CHARACTERISTICS

A great deal has been written concerning microwave energy and radiometry; consequently, a detailed account will not be presented here.[4] However, for completeness, some salient features of microwave radiometry will be discussed.

In general, microwave radiometry (MICRAD) sensors are passive and respond to electromagnetic radiation ranging in wavelength from approximately 0.1 mm to 30 cm. This is the same region of the electromagnetic spectrum in which radar operates. However, unlike radar, MICRAD does not transmit any radiation, but receives the natural electromagnetic radiation emanating from all bodies in the universe due to the heat energy within the body. Fundamentally, MICRAD operates in the same manner as infrared radiometry, but practical differences arise because of the large difference (approximately 10^4) in wavelength used by

these sensors. MICRAD systems can operate day or night and in almost all weather conditions, providing a proper operating frequency is chosen (usually <20 GHz, 35 GHz, or 94 GHz). Weather penetration and image tone density (apparent brightness temperature) contrast of objects within these microwave "windows" decreases as the frequency increases. Conversely, spatial resolution (for a physically fixed antenna size) increases as the frequency increases. The atmospheric window which exists at 35 GHz is frequently chosen because it results in a good tradeoff between the weather penetration of the band <20 GHz and the better spatial resolution obtainable with reasonably sized antennas at 94 GHz. In a comparison with visible and infrared imaging systems, MICRAD systems operating in any of these windows (especially the <20 GHz and 35 GHz windows) experience orders of magnitude less attenuation in clouds and fog than visual and thermal infrared (IR) sensors. Excellent MICRAD images of terrain features have been obtained through cloud cover and through light rain at 8.9 mm wavelengths.[5]

The physical characteristics of the MICRAD system which generated the images used in connection with the experiment reported here are listed in Table 1.[6] Figure 2 is a schematic diagram of a scanning system illustrating the geometry associated with image acquisition and depicting the way in which the MICRAD imagery used in this study was acquired. Images are generated by scanning the MICRAD system's antenna beam over the terrain. The imaging MICRAD system is installed in a Rockwell International OV-10 aircraft. Three rotating parabolic antennas collect data by scanning a strip of ground perpendicular to the flight path of the aircraft. Forward motion of the aircraft provides for successive scanning along the direction of flight. The width of the scan is four times the altitude of the aircraft above the terrain.

In order to produce a visual representation of the MICRAD scene, the scanning is repeated in the laboratory with a visible light modulated by the intensities in the MICRAD images; the resulting visual rendition of the MICRAD "picture" is recorded on film. There are geometrical distortions in the images generated with the present system and these are given. The antenna scans the terrain with a tangential function of time; but the processor scans with a linear function of time. Consequently, the images are reasonably correct only within the center third of the picture where the tangent of the scan angle is approximately equal to the scan angle. Measurements made in connection with our experiments were accomplished by utilizing this center strip of the image product.

The image tone at each point in a MICRAD image is determined by the amount of microwave energy emanating from the corresponding point on the ground. Microwave energy emanating from a material on the earth's surface is composed of the sum of three components (Figure 3). Associated with the three components of microwave energy are three unitless quantities called

TABLE 1. 35 GHz MAPPING SYSTEM CHARACTERISTICS

Mount	Unstabilized
Number of Antennas	3
Antenna Type	Cassegrain
Antenna Diameter	0.508 m (2 feet)
Antenna Polarization	Horizontal
Beam Incidence Angle	30 degrees
Beamwidth (3 db)	1.1 degrees
Beam Intercept Width-Center Scan	5.6 m/250 m (22′/1000′)
Beam Intercept Length-Center Scan	6.6 m/250 m (26′/1000′)
Scan Angle	120 degrees
Scan Width	1010 m/250 m (4000′/1000′)
Scan Rate Range	0.4 – 12 scans/sec
Radiometer Type	Dicke/Hybrid
Switch Point—Dicke to Hybrid	11 scans/sec
System Losses	2.7 db
R.F. Amplifier Noise Figure	3.0 db
System Noise Figure	5.7 db
Frequency	33.6 GHz
R.F. Bandwidth	500 MHz
Integration Time Range	0.7 – 21 Msecs
System RMS Sensitivity (T=1 sec)	0.15° K

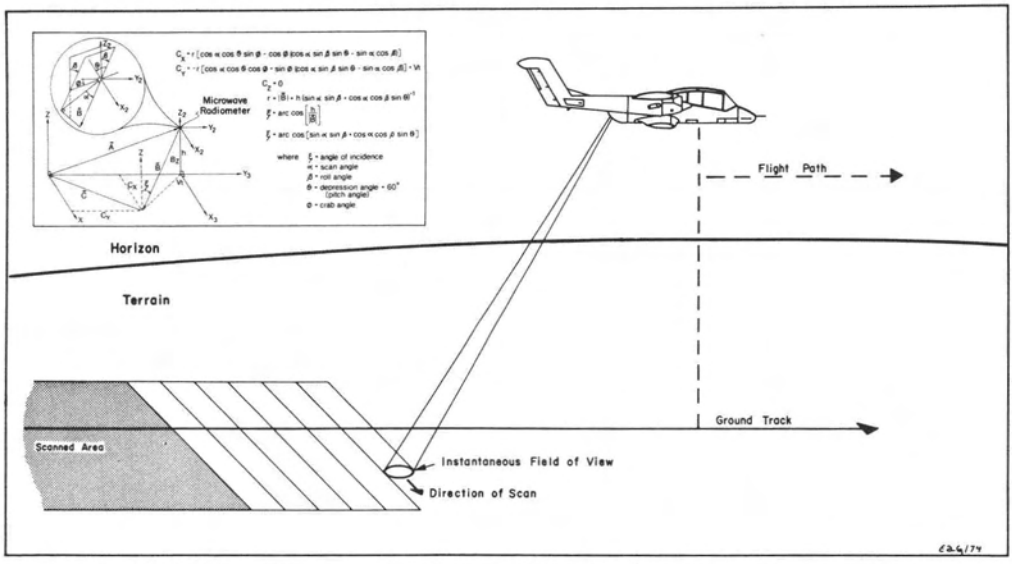

FIG. 2. The MICRAD system, mounted in an OV-10 aircraft, scans terrain in successive swaths perpendicular to the direction of flight. The width of single scan and the instanteous spot size (field-of-view) are functions of aircraft altitude. Insert depicts detail of scan geometry. From a comparison of the insert diagram and material contained in Table 1, calculations of variance in beam incidence angle can be made.

emissivity (ϵ), reflectivity (ρ), and transmissivity (τ). The sum of these quantities is equal to one. The emissivity of a body is a measure of how well the body approximates the theoretical black body, for which the emissivity is one. Emissivity, then, is the ratio of the energy emanating from a black body and that emanating from the body in question at the same absolute temperature as the black body. Reflectivity is the ratio of incident energy to reflected energy. Transmissivity is the ratio of incident energy to energy passing through the body.

The quantities of emissivity, reflectivity, and transmissivity are related to the material constituents of a body, its shape, the frequency of observation, and, to some extent, its temperature and other physical parameters such as density. For example, the emissivity of water and sandy soil at 10 GHz for horizontal polarization (the polarization which is used with the imaging system discussed) are respectively 0.347 and 0.927. In most cases, terrestrial objects are opaque to microwave radiation. This means that for most objects in our environment the transmitted component of their microwave response is relatively unimportant. Transmissivity for water is essentially zero and for dry sandy soil is very small for thicknesses greater than a few hundred centimeters (see below). If we assume the transmissivity is zero, then the reflectivity for water is $1 - 0.347 = 0.653$ and for sand is 0.073. A good emitter then is a poor reflector, and conversely a good reflector is a poor emitter. Examples of transparent material in the microwave are snow, the atmosphere and clouds are very transparent they are very poor emitters of microwave energy. The only significant celestial microwave source is the sun which emits little microwave energy in comparison to visual and infrared energy (see Figure 4).

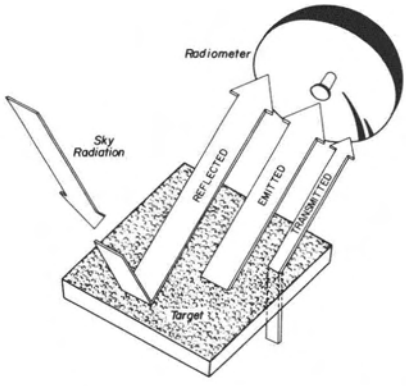

COMPONENTS OF MICROWAVE RADIATION

FIG. 3. Microwave radiation mapped by the system is derived from energy reflected, emitted, and transmitted from surface objects. Typically, the transmitted component is very small. Reflectance and emittance combine to produce characteristic tonal and textural patterns which can be used to detect and identify surface phenomena.

Consequently, the sky is always very cold. That is, the sky emits very little energy at microwave wavelengths unless we look directly at the sun. Sky temperatures at 33.6 GHz will vary from approximately 15°K for clear air to about 100°K for foul weather (rain and clouds). The importance of the cold sky at these microwave frequencies is that a large radiometric contrast will exist between objects of different reflectivity even though both objects may have the same physical temperature. The cold sky temperature and the fact that, in general, the terrain physical temperature will vary only about 10 percent on an absolute scale allow the target characteristics of emissivity and reflectivity to dominate the MICRAD signal response from a given scene (again assuming transmissivity is zero).

It is common practice in radiometry to consider temperatures of targets instead of electromagnetic power emanating from a target. This eliminates system characteristics. In microwave radiometry, the power received is directly proportional to the first power of the absolute temperature; in the IR band the power is directly proportional to the fourth power of the temperature of the target. This makes infrared considerably more sensitive to terrain temperature changes than in MICRAD. The microwave radiometric brightness temperature (T_r) is given by

$$T_r = \epsilon T_1 + \rho T_2 + \tau T_3$$

where T_1 = target physical temperature,
T_2 = temperature of reflected source (usually sky temperature), and
T_3 = radiometric temperature of source transmitted through target.

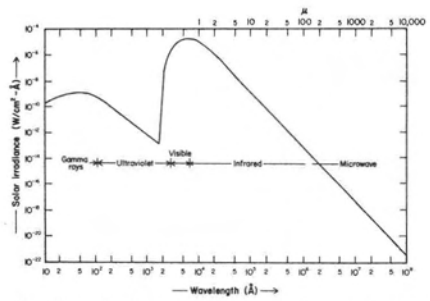

FIG. 4. Graph showing solar energy at the earth's surface after attenuation by atmospheric effects. Note the logarithmic axes. An atmospheric window of about 0.89 cm allows a slightly larger amount of energy to reach the ground surface than shown here; this amount, however, is quite small.

In order to illustrate some of the features of MICRAD discussed, assume that sand and water are both at 20°C (68°F). Then we have for the brightness temperatures:

$$T(\text{sand}) = 0.927\ (293) + 0.073(15) = 271°\text{K}$$

$$T(\text{water}) = 0.347\ (293) + 0.653(15) = 111°\text{K}$$

This results in a radiometric contrast of 160°K. Now if we assume the sand heats up to 50°C (122°F), about a 10 percent increase, the brightness temperature of the sand is about 300°K, a change of 29°K. In normal operations, contrasts due to changes in reflectivity can be greater than those illustrated here, because the reflectivity of metal surfaces approaches one.

Methodology

Test sites for the research reported here are located on the West Side of the San Joaquin Valley, California. Between March, 1973 and July, 1974 two transects, each approximately 32 km long and 1.6 km wide, were imaged several times. As research progressed it became increasingly clear that soil moisture, particularly surface soil moisture, was an important factor influencing the MICRAD response of bare, unvegetated terrain. In an attempt to isolate the effect of varying soil moisture content on microwave emission, ground truth data designed to test this relationship were collected coincident with MICRAD image acquisition. The test site for this analysis was narrowed to a single transect of 45 agricultural fields, each approximately 0.8 km on a side, near Lost Hills, California. Figure 1 shows the Lost Hills test area as photographed by a National Aeronautics and Space Administration (NASA) high-altitude aircraft. The photograph has been annotated to show the soil types in the transect area and the relative location of the study area within California. Irrigation agriculture is wide spread here. Thus, a variety of soil moisture regimes may typically be encountered on any given date.

Coincident with a MICRAD overflight, which took place on February 20, 1974, 29 soil samples were taken from the top 5 cm of unvegetated fields. Because of the nature of the total range of data being acquired coincident with image acquisition, only one sample per field was obtained. We feel this was a handicap especially when examining the correlations obtained from higher altitude and large instantaneous field-of-view images, as will be discussed later. MICRAD images (Figures 5 and 6) were acquired from altitudes of 2500 feet (760 m) and 6500 feet

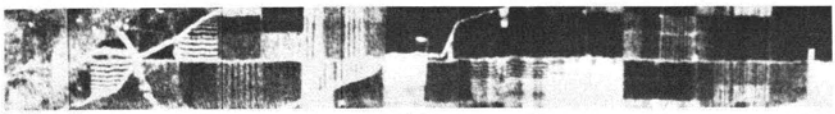

FIG. 5. A MICRAD image of a portion of the Lost Hills test site taken from 2500 feet (760 m) on February 20, 1974. Soil samples from 29 locations were correlated to tones from this image. Obvious differences in soil moisture content may be seen in several areas where strip irrigation produces alternating rows of wet (light) and dry (dark) soil. More subtle variations in soil moisture are detectable by examining the image with a microdensitometer.

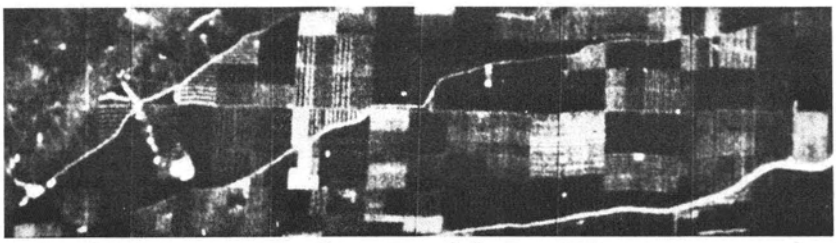

FIG. 6. This MICRAD image of a portion of the Lost Hills test site was produced shortly after the image shown in Figure 5. The altitude shown here is 6500 feet (1980 m). The resolution decays with increasing flight altitude as does the soil moisture/image tone relationship.

(1980 m) at the time soil samples were collected. The precise location of each sampling point was noted on black-and-white aerial photos of the area. At the same time the surface roughness of each field was also evaluated using a subjective five step scale. Roughness ranged from smooth graded fine textured surfaces (1) to cloddy furrowed surfaces (5). Row spacings of all fields sampled which were furrowed was 3 feet. The direction of these furrows were either north-south or east-west, that is, parallel or perpendicular to the OV-10 flight line which was north-south.

The moisture content of the samples taken was determined by weighing the individual samples both before and after oven drying. Soil moisture is expressed as a percentage of dry weight by using the formula

$$\frac{\text{wet weight} - \text{dry weight}}{\text{dry weight}} \times 100$$

The error associated with this technique is minimal, on the order of less than 1 percent of the dry weight. In order to correlate the soil moisture content to the microwave imagery, the image tone, or optical density (an approximation of brightness temperature), was measured for each sample location using a microdensitometer. Transmission density readings were taken from photographic copy negatives of the microwave images. This was done because precise comparative density measurements are difficult to obtain from the photographic print data format produced as the system's output. In addition, when transferring the image from a print format to negative transparency material, a 12-step grey wedge was inserted. This insures that image tone densities from different altitudes, times, or dates can be normalized.

Discussion and Results

Figure 7 shows the scatter plot produced by pairing the data from each soil moisture sample with the brightness temperature produced at 2500 feet (760 m). A best-fit line, indicating the relationship between the two variables, was calculated by the least

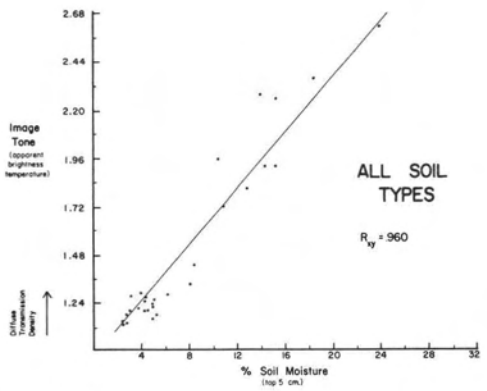

FIG. 7. Correlation of image tone (vertical axis) and soil moisture content from the top 5 cm (horizontal axis). The data were derived from the February 20 MICRAD image (Figure 5). The least-squares method of regression analysis was used to produce the best-fit line.

squares method. The equation for this relationship is $y = 0.07\ x + 0.97$ where x is the percent of soil moisture by weight and y is the diffuse transmission density. The Pearson product-moment correlation coefficient (r_{xy}) for these data is 0.960, indicating a strong positive correlation between soil moisture and image density. In this test, then, 92.0 percent of the variation in y (diffuse transmission density) can be attributed to the variation in x (soil moisture), leaving less than 8 percent to be explained by other variables.

The value of 0.960 for r_{xy} indicates that a very strong relationship exists between the two variables, soil moisture and diffuse transmission density. An F test was performed to test the linearity of the regression line as measured by r. A computed F value of 324.871 with 27 minus one degrees of freedom, indicated that a linear relationship exists in the data at the 0.001 level of significance. In addition to this relationship, recent work has indicated that soil type and particle size composition also may affect brightness temperature.[7] In order to test the effect of these variables, soil information for the test transect was gathered and analyzed. The United States Soil Conservation Service has mapped two soil types within the test site (Figure 1). The San Emigdio-Hisperia association consists of well-drained and moderately coarse material derived from sedimentary and granitic sources. The Panoche association is composed of medium textured alluvial soil produced from sedimentary parent rock.[8] The fundamental difference between the two soil types in the test site relates to the particle size composition, which is felt to effect emission properties as well as the behavior of water within the soil itself. For example, hydraulic conductivity is greater for coarse material and one might expect more rapid infiltration of irrigation water and more rapid drying shortly after water application. The coarser San Emigdio formation would therefore be expected to exhibit a higher emissivity due to a drier surface layer.

The data that paired soil moisture with transmission density were segregated into two sets representing the soil types present, and new scatterplots were produced (Figure 8). Again, regression lines were fitted by the least squares method. The coarse-grained San Emigdio soil produces a coefficient of correlation slightly lower than the correlation for the ungrouped data $r_{xy} = 0.958$. The medium-textured Panoche soil shows a higher correlation $r_{xy} = 0.982$, a fact which

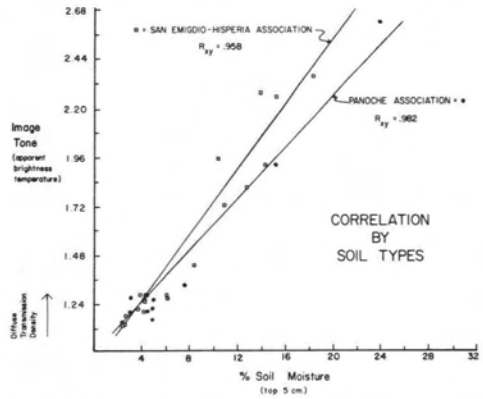

FIG. 8. When data are segregated into two groups by soil types, the best-fit regression line conforms to points more closely. Coefficients of correlation improve somewhat when the data are divided in this manner.

tends to support somewhat the hypothesis that water content in the top 5 cm is more uniform with depth for finer grained soils. Although the regression lines produced by these correlations have slightly different slopes it is difficult to make conclusive statements concerning the difference between the two lines. Owing to the small number of samples for each soil type, there is little evidence indicating that these regression lines are significantly different, the standard normal probability being 0.797. Tests of these regression lines using the F statistic again indicate that a strong linear relationship exists in the data at the 0.001 level of significance.

Given the number of samples acquired in this experiment, statements concerning a relationship between surface roughness and brightness temperature are difficult. By grouping soil samples into smaller classes of similar surface roughness, computer-generated correlations of soil moisture and diffuse transmission density show regression lines of almost equal slope and y-intercept for each of the surface roughness classes present. Assuming that deviations from the regression equation are normally distributed within each group, the probability of significant differences in these lines is very low. This is particularly the case where soil moisture is low (below 10 percent). When soil moisture approaches saturation, surface roughness appears to produce an effect on transmission density. The data are not conclusive, however, and this is one area where more study and sampling are needed.

Images obtained from 6500 feet (1980 m) are, predictably, poorer in resolution and

provide less evidence of linear expression of the transmission density/soil moisture relationship. The coefficient of correlation with images from this altitude is about 0.70, which shows a much weaker covariance. This decrease in linear relationship may be, in part, the result of system's resolutions. That is, the higher the altitude of the sensor platform, the greater the potential for variation in the microwave energy which is emanating from a given scene as it is integrated to a single value over larger areas. Further, the soil moisture variation in a very small area of the type of fields sampled in this experiment based on our results does not appear great (remembering that extreme care was taken to collect the image density information at the exact spot the sample was taken). However, because a large area is included in the instantaneous field-of-view of the system, the number of samples required to adequately portray the soil moisture should also increase. For example, in the experiments discussed here the instantaneous spot size of data taken at 6500 feet (1980 m) cover approximately 675 percent more area than data acquired at 2500 feet (760 m). This makes accurate correlation with point sample data more difficult. More testing with a higher density of sampling sites per field is required to adequately determine the validity and significance of this relationship. Recent studies by Blanchard and Ulaby indicate that as many as 30 to 36 stratified surface samples per 40-acre field may be required to adequately characterize surface soil moisture of such fields where the system's resolution element is the whole field.[9]

Conclusions

Based on our analysis of the data produced by the imaging passive microwave radiometer discussed here, we have shown that a statistically highly significant linear correlation exists between diffuse transmission density and moisture content of the top 5 cm of the soil. Further, this relationship appears to intensify when the data were segregated by soil type. Conclusive evidence of the effect of surface roughness on transmission density temperature was not found. However, based on these experimental results and on the work of Schmugge *et al.* (1974), mineralogy and soil particle size do appear to have an effect on diffuse transmission density. Other researchers working with passive microwave radiometers have not had the benefit of access to data from an imaging system such as the one which produced these results. The relatively high-resolution imagery produced by this system greatly facilitated our analysis.

From our experiments conducted to date, it appears that imaging MICRAD systems do have a potential for providing information to agriculturalists, meteorologists, hydrologists, and other environmental scientists interested in obtaining areally extensive data concerning near surface soil moisture conditions. Clearly, considerably more testing is required and, as more data is acquired, the relationships will be further tested and refined.

Acknowledgments

This research was performed under contract to the Department of the Navy/Naval Weapons Center, China Lake, California (Contract N00123-73-C-2352).

References

1. Moore, R. P., 1974, "Microwave Radiometric All-Weather Imaging and Piloting Techniques," NATO Conference Pre-Print, No. 148 on Guidance and Control of V/STOL Aircraft and Helicopters at Night and in Poor Visibility, AGARD, Nenilly Sur Seine, France, 10 pp.
2. Poe, G. A., 1971, "Remote Sensing of the Near-Surface Moisture Profile of Specular Soils with Multi-Frequency Microwave Radiometry," *Proceedings of the Society of Photo-Optical Instrumentation Engineers,* Vol. 27, pp. 135-145.

   Blanchard, B. J., 1972, "Measurements from Aircraft to Characterize Watersheds," paper presented at 4th Annual Earth Resources Program Review, NASA, Lyndon B. Johnson Space Center, Houston, Texas, January 17-21, 1972.

   Blinn, J. C., III, J. E. Conel, and J. G. Quade, 1972, "Microwave Emission from Geological Materials: Observations of Interface Effects," *Journal of Geophysical Research,* Vol. 77, no. 23, pp. 4366-4378.

   Blinn, J. C., III, and J. G. Quade, 1972, "Microwave Properties of Geologic Materials," paper presented at 4th Annual Earth Resources Program Review, National Aeronautics and Space Administration, Lyndon B. Johnson Spacecraft Center, Houston, Texas, January 17-21, 1972.

   Schmugge, T., P. Gloersen, T. Wilheit, and F. Geiger, 1974, "Remote Sensing of Soil Moisture with Microwave Radiometers," *Journal of Geophysical Research,* Vol. 79, no. 2, pp. 317-325.
3. Poe, G., A. Stogryn, and A. T. Edgerton, 1971, "Determination of Soil Moisture Content Using Microwave Radiometry," Final Report 1684FR-1 DOC Contract 0-35239 Aerojet-General Corporation Microwave Division, El Monte, California.
4. For more information concerning microwave energy and radiometry the reader is referred

to Harris, D. B., 1960, "Microwave Radiometry," *Microwave Journal*, April, pp. 41-45.

Hooper, J. O., J. W. Battles, 1963, "Some Calculations of Target Temperatures in Microwave Radiometry," Naval Ordinance Laboratory, Cornona, California, NAVWEPS Report 8140, March 15, 106 pp.

Kraus, J. D., 1966, *Radio Astronomy*, McGraw-Hill, 481 pp.

Taylor, H. P., 1967, "Radiometer Equation," *Microwave Journal*, May, pp. 39-42.

Evanisko, F. E., 1974, "Evaluation of the Information Content of Passive Microwave Radiometric (MICRAD) Data for the Detection and Identification of Urban and Rural Terrain Features in the West Side of the San Joaquin Valley, California," Progress Report, Department of the Navy, Contract N00123-73-C-2352, June 30, 47 pp.

Reeves, R. G., (ed. in chief), 1975, *Manual of Remote Sensing*, Falls Church, Virginia, American Society of Photogrammetry, especially chapters: 4, "Interaction Mechanisms;" 9, "Microwave Remote Sensers;" 14, "Fundamentals of Image Interpretation;" and 22, "Crops and Soils."

Lintz, J., Jr. and D. S. Simonett (eds.), 1976, *Remote Sensing of Environment*, Addison-Wesley, Reading, Massachusetts, chapter 6, "Passive Microwave Systems," pp. 194-233.

5. Brunelle, D. N., J. E. Estes, M. R. Mel, R. R. Thaman, F. E. Evanisko, R. P. Moore, C. A. Hawthorne, and J. O. Hooper, 1974. "The Usefulness of Imaging Passive Microwave for Rural and Urban Terrain Analysis," paper presented at the 9th International Symposium on Remote Sensing of Environment, Ann Arbor, Michigan, April 15-19, 1974.
6. Moore, R. P., and M. C. Hoover, 1971, "An Airborne Ka-Band Microwave Radiometric Measurement Mapping System," Proceedings of the Society of Photo-Optical Instrumentation Engineers, Vol. 27, pp. 147-156.
7. Schmugge, *et al.*, *op. cit.*, footnote 3, pp. 317.
8. United States Department of Agriculture, Soil Conservation Service, 1967, "Report and General Soil Map of Kern County, California," Bakersfield, California, September, pp. 15-16 and 24-25.
9. Blanchard, B. J., and F. Ulaby, 1977, personal communication.

Optical Science and Engineering

The Optical Science & Engineering Short Course will be given at the Doubletree Inn in Tucson, Arizona by members of the faculty of the Optical Sciences Center, the University of Arizona, 3-13 January, 1978. The purpose of the course is to acquaint both the specialist and the nonspecialist engineer or scientist with the latest techniques in the design and engineering of optical systems. The course comprises 19 three-hour lectures, accompanied by detailed notes.

In support of the general subject there will be discussions on a wide range of topics: Geometrical and physical optics, optical system layout and design, Fourier methods, photodetectors, polarized light, radiometry and photometry, image quality, adaptive optics, optical testing, lasers, infrared systems, photographic and electro-optical systems, remote sensing methodology, sampled imagery and digital image processing, and holography and data processing.

Inquiries should be addressed to

Professor Philip N. Slater
Optical Systems and Engineering Short Courses Inc.
P.O. Box 18667
Tucson, Arizona 85731